Supplementary Information

Materials

The following details on materials and methods are contained in the Supporting Information: chemicals, synthesis, and characterization of dimer-enhanced fluorescent probes.

Gold (III) chloride trihydrate ($HAuCl_4 \cdot 3H_2O$, SCR) 49%, Sodium citrate (SC, Aladdin) ≥ 99.9%, Dopamine hydrochlonde (PDA, sigma), (3-Aminopropyl) triethoxysilane (Aladdin) 99%, Tris (hydroxymethyl)aminomethane (SCR), Tetraethyl orthosilicate (Aladdin), sulfo-Cy5 amine (duofluor), Phosphate buffered salt solution (PBS) and HeLa cells were provided by keygen-BioTECH. Ultrapure water was obtained from a Milli-Q water purification system (Millipore Corp., Bedford, MA) with resistivity of 18.2 MΩ cm and used for all procedures.

Test instrumentation

TEM images were acquired from a transmission electron microscope (Hitachi HT7700) at an acceleration voltage of 100 kV. UV-visible spectrophotometer Model: Shimadzu UV3600 purchased from Shimadzu Company. SEM imaging was performed by a field-emission scanning electron microscope (S-4800, Hitachi Japan) at 5 kV. The DFM images, SPR scattering spectrum measurements were recorded by an inverted microscope (eclipse Ti-U, Nikon) equipped with a monochromator (Acton SP2358), a −75 °C cooled CCD detector (PIXIS 400BR: excelon, Princeton Instruments) and a 633 nm continuous-wave laser light (Spectra-Physics Excelsior, 100 mW). The microscope was equipped with a 60× objective lens, a dark field condenser (0.8 < numerical aperture (NA) < 0.95), and a true-color digital camera (Nikon DS-fi2). The spectra were integrated through a 1 μm slit width. Heating digital display Zili agitator Model: SHT-19T purchased from joanlab Company; Ultrasonic cleaner type: SK2200H purchased from Shanghai Science Guide; Electronic balance model: BSA124S from Sartorius; Centrifuge model: H1650 purchased from Xiangyi; Two-photon laser confocal microscope: LSM880 from ZEISS.

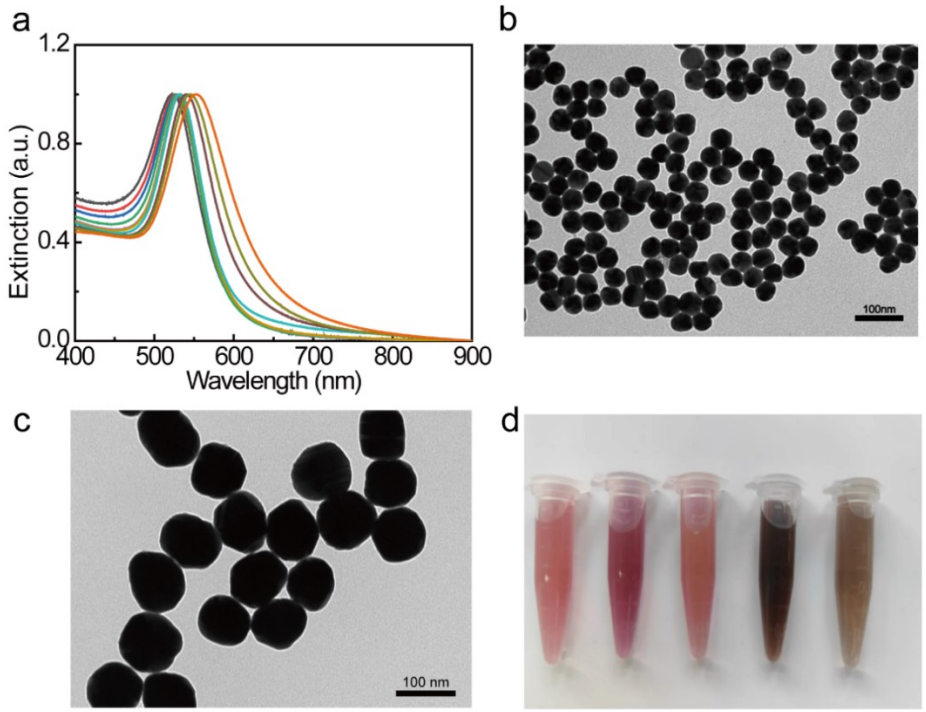

Figure S1 (a) Normalized plot of UV-vis extinction values of different sizes of gold nanoparticles. (b) TEM plot of 45 nm AuNPs. (c) TEM plot of 90 nm AuNPs. (d) From left to right are: 45 nm AuNPs; Dimer (post-centrifugation); 90 nm AuNPs; PDA+ Dimer (pre-centrifugation); PDA (post-centrifugation).

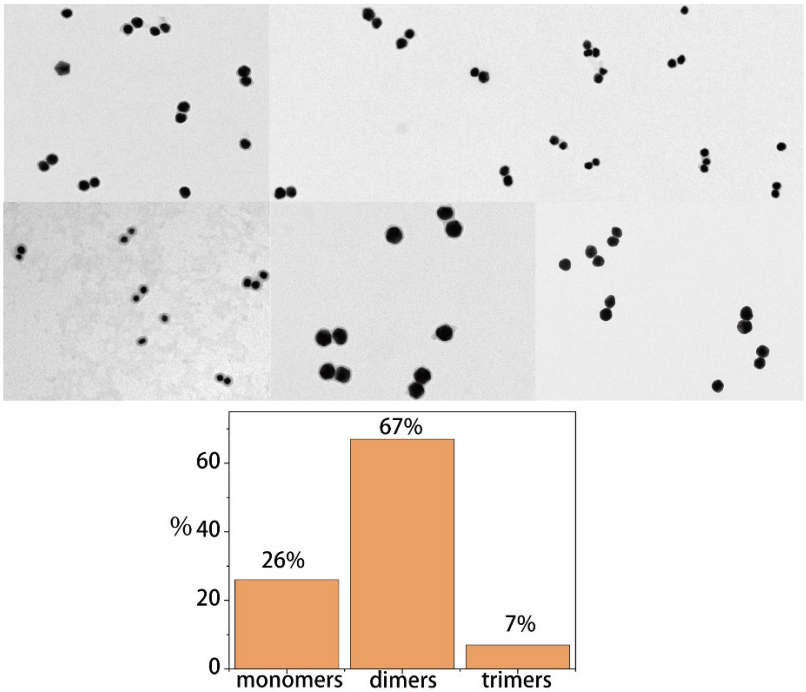

Figure S2 multiple TEM plots used to do dimer yield statistics.

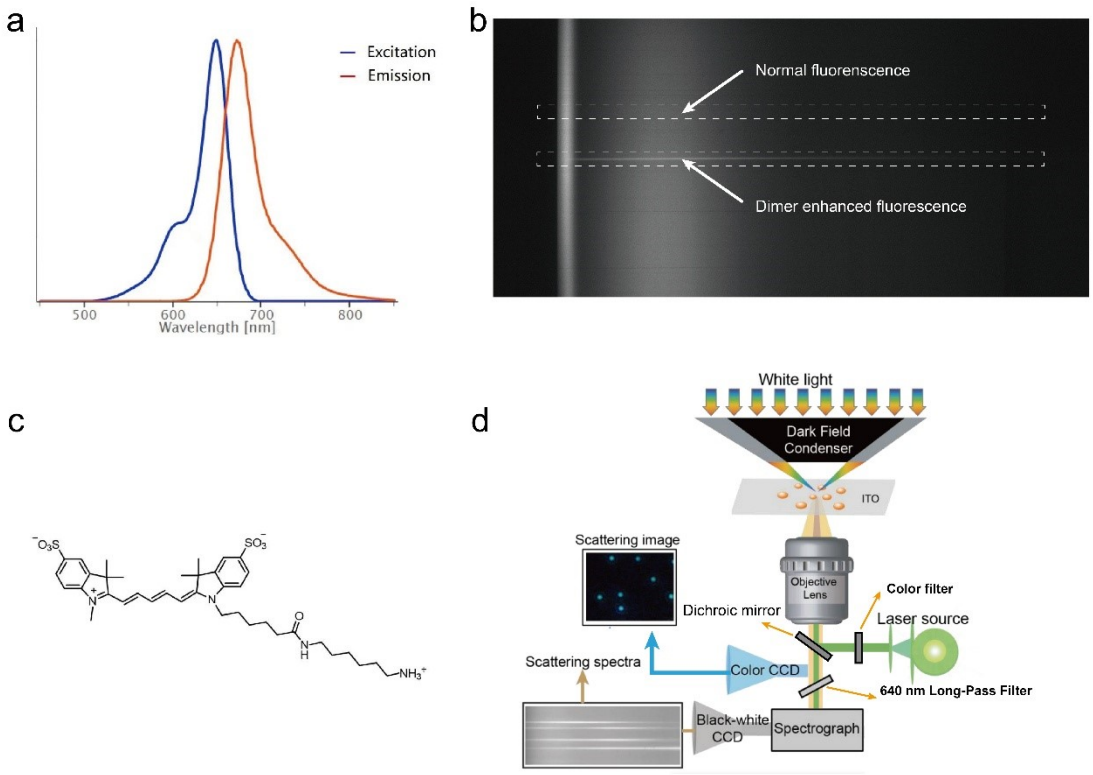

Figure S3. (a) Excitation and emission spectra of the fluorescent molecule Cy5. (b) Comparative diagram of the effect of gold nanoparticle dimers on the luminescence of the fluorescent molecule in the slit. (c) Structural formula of the fluorescent molecule. (d) Schematic diagram of DFM microspectral system.

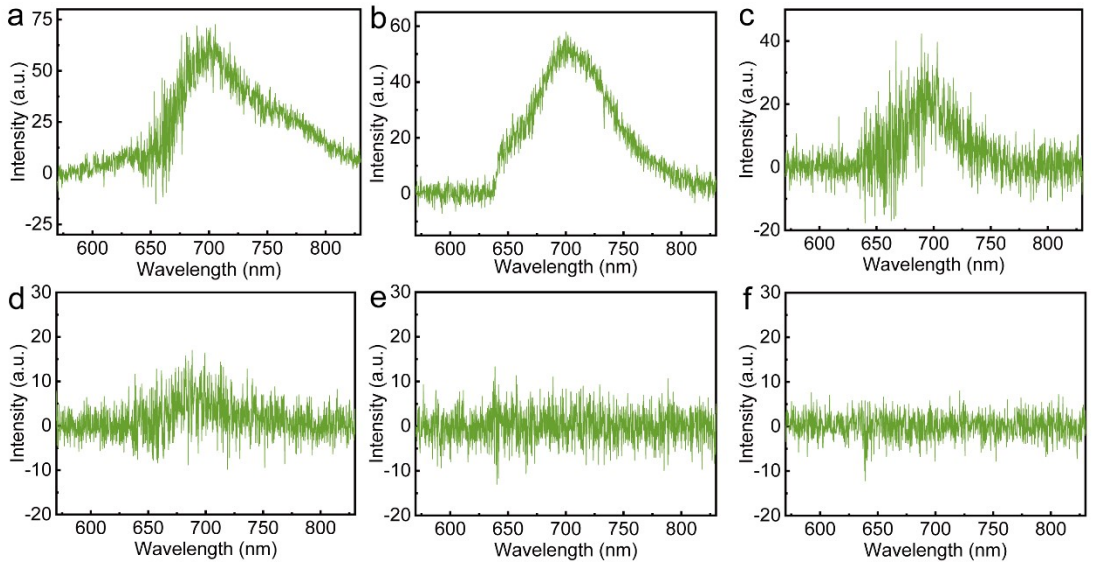

Figure S4. Fluorescence intensity profiles of dimers(a,b,c) and monomers(d,e,f) at different fluorescent molecule concentration(a,d：6×10^{-6} M. b,e：3×10^{-6} M. c,f：1×10^{-6} M.)s.

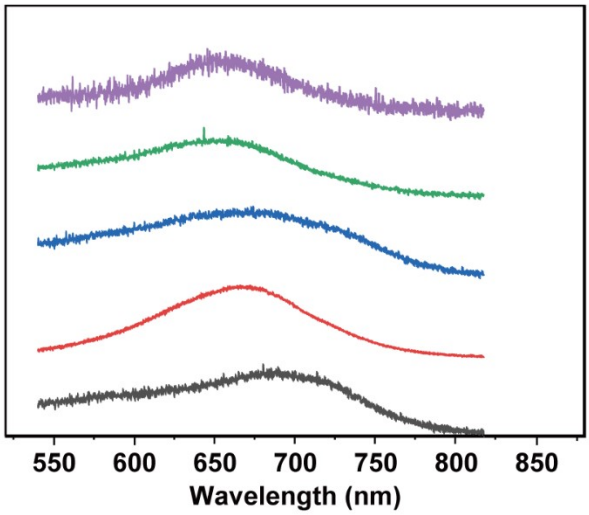

Figure S5. LSPR peaks of multiple fluorescent probes in (Fig. 4a) .

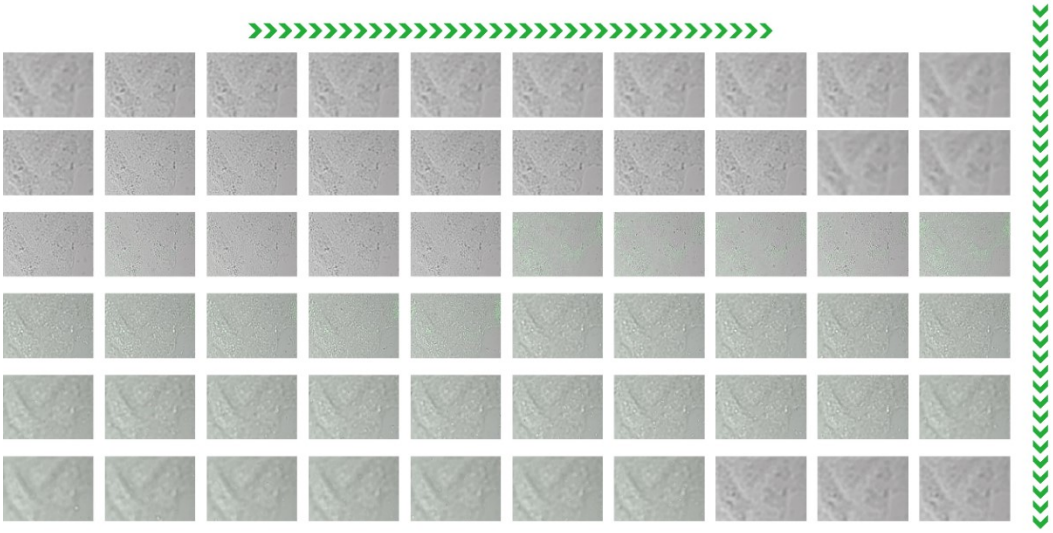

Figure S6. Confocal microscopy longitudinal scanning image of the cell z-axis, centered on the plane with the highest number of individuals in positive focus of the dimer particles, 30 µm above and below and 1 µm apart.

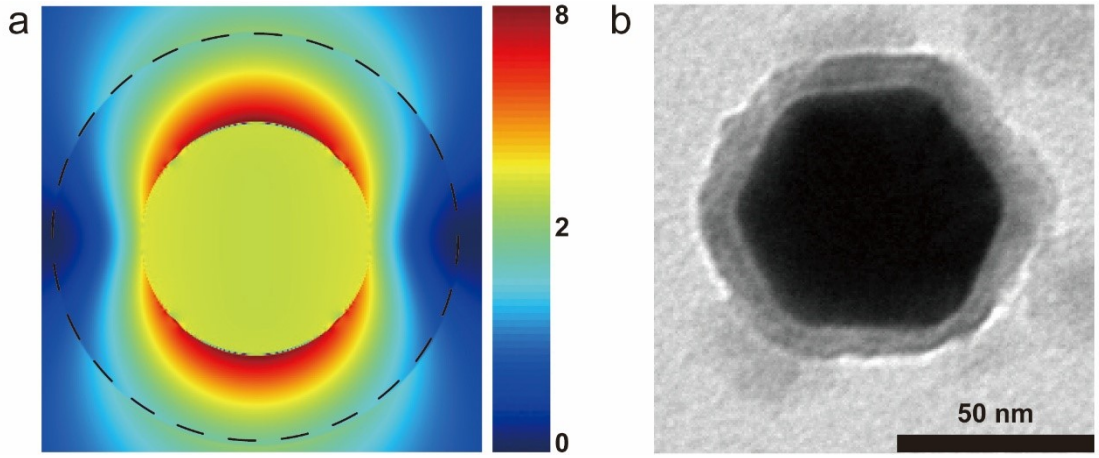

Figure S7. (a) FDTD simulates the electric field strength of the monomer. (b) TEM image of monomer encapsulated with mesoporous silica shell.

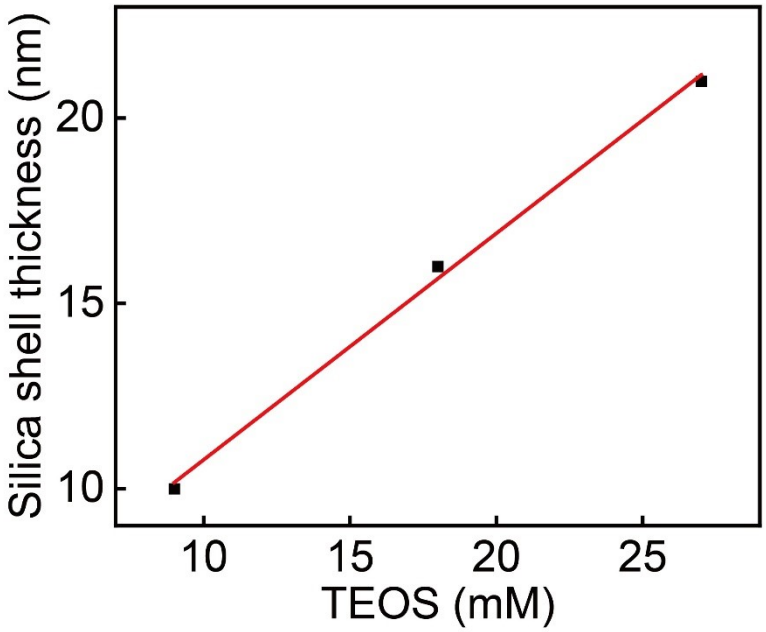

Figure S8 The relationship between TEOS concentration and silica shell thickness